ACS OMEGA

http://pubs.acs.org/journal/acsodf
Article

Protruding Boron Nitride Nanotubes on the Al_2O_3 Surface Enabled by Tannic Acid-Assisted Modification to Fabricate a Thermal Conductive Epoxy/Al_2O_3 Composite

Zahid Hanif, Duy Khoe Dinh, Arni Gesselle M. Pornea, Numan Yanar, Min Seok Kwak, and Jaewoo Kim*

Cite This: *ACS Omega* 2024, 9, 38946−38956
Read Online

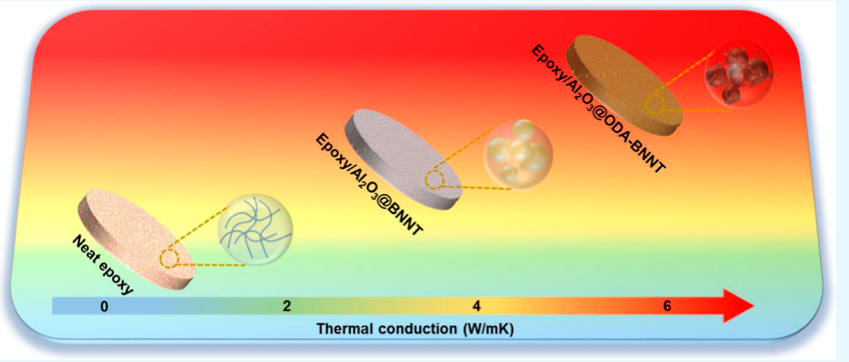

ABSTRACT: Over the past few years, the ability to efficiently increase boron nitride nanotube (BNNT) production has opened up ample research possibilities. BNNT has garnered significant attention for diversifying its industrial applications. However, the problem of poor processability resulting from agglomeration and uneven distribution has emerged as a major challenge to integrating BNNT into the polymer matrix for composite material formation. Utilizing noncovalently attached molecules with various reactive sites can be a logical method to enhance the compatibility of BNNT with different polymers. The present study explored a simple approach to protruding BNNT onto the surface of Al_2O_3 through tannic acid (TA)-assisted generation of alkyl chains (octadecylamine, ODA) to fabricate Al_2O_3@ODA-BNNT. The subsequent compounding of Al_2O_3@ODA-BNNT with epoxy polymer generates interconnected thermal conduction pathways, thereby improving the thermal conduction and mechanical performance of the composites. The current research approach allows for the even distribution of BNNT throughout the polymer matrix, as demonstrated by optical characterization, mechanical performance analysis, and isotropic thermal conductivity analysis. The fabricated epoxy composite by incorporating a 2 wt % (BNNT = 1.3 wt % and ODA = 0.7 wt %) ODA-BNNT exhibited 5.117 W/mK thermal conductivity and 7.43 MPa mechanical stress. Thermal conductivity improved by 2528, 76.56, and 54.7%, while mechanical stress enhanced by 270, 221, and 34% compared to neat polymers without BNNT and virgin BNNT epoxy composites, respectively.

1. INTRODUCTION

The rise in heat generation in contemporary electronic devices as a result of miniaturization, integration, and high power density has emerged as a significant challenge.[1−3] The buildup of heat poses negative effects on the stability, safety, efficiency, and lifespan of electronic devices.[4] Developing thermal management materials (TMMs) with high thermal conductivity to effectively dissipate generated heat from electronic devices is both challenging and crucial.[5,6] Polymers, including polyethylene, polyurethane, silicon, and epoxy resin,[7−10] have been utilized in the development of TMMs due to their lightweight, ease of processing, cost-effectiveness, electrical insulation, and thermal stability.[11,12] Epoxy resin has been extensively utilized in electronic devices due to their exceptional electrical insulation, easy fabrication, high dielectric constant, bonding properties, and chemical resistance.[13] The aforementioned properties make them highly promising for achieving the necessary heat flux in electronic devices.[14−16] Nevertheless, the heat conduction of polymers in their pure forms is relatively low, ranging from 0.1 to 0.5 W/mK. This limited heat dissipation capability prevents their widespread

Received: June 6, 2024
Revised: August 18, 2024
Accepted: August 28, 2024
Published: September 5, 2024

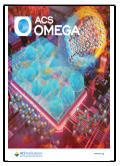

https://doi.org/10.1021/acsomega.4c05323
ACS Omega 2024, 9, 38946−38956

use in the electronic industry, where there are strict demands for efficient heat dissipation.[17,18]

Using thermally conductive fillers to create polymer composite materials is a widely used method to enhance the thermal conduction of polymers.[19] Various fillers, such as carbon materials, metal particles, functionalized graphene, and ceramics, have been chosen to improve the thermal conductivity of polymers.[20−25] Carbon materials such as carbon nanotubes, graphene, and graphite have demonstrated high thermal conductivity in polymer composites.[26,27] However, their significant lower electrical insulation, which is essential for electronic packaging, restricts their widespread utilization. In contrast, different inorganic fillers, including boron nitride (BN),[28,29] boron nitride nanosheet (BNNS)[30] silicon carbide (SiC),[31] aluminum nitride (AlN),[32] spherical aluminum oxide Al_2O_3,[33] and alumina platelets,[34] have been applied to form electrically insulating yet highly thermal conduction composites. These fillers are incorporated into the polymer matrix to create heat conduction paths to dissipate heat effectively during subsequent device operation. For Al_2O_3-filled polymer composites, high loading is required to achieve high thermal conduction.[35−37] High loading of fillers into the polymer matrix increased the interfacial thermal resistance; consequently, thermal conductivity was hampered.[38] Improving thermal conductivity poses a significant challenge due to the lack of efficient thermal conduction pathways. Moreover, excessive use of microfillers can negatively impact polymer composites processability and mechanical strength.[39]

Incorporating a small fraction of nanofillers with the main Al_2O_3 filler into the matrix is an effective method that enhances the thermal conductivity of polymer composites while also preserving their processability and mechanical performance.[40] In recent years, boron nanosheets (BNNS) and boron nanotubes (BNNT) have gained immense attention due to their intrinsic high thermal conductivity, chemical stability, and neutron shielding.[41] BNNS can be formed by both bottom-up growth and top-down exfoliation to form a 2D sheet structure, whereas BNNT can be synthesized through the nucleation and growth of boron and nitrogen-containing precursor materials that bestow it 1D tubular structure.[42] BNNT stands out among other fractional fillers, including BNNS, due to its unique 1D structural feature.[43] Due to the tubular structure, even a small amount of BNNT (0−2 wt %) has a high tendency to form a 3D network in the presence of co-fillers to enhance the overall performance of composites.[44] BNNT, however, has limited dispersion in solvents and tends to agglomerate in the polymer matrix due to strong van der Waals interactions.[45,46] This leads to an increase in interfacial thermal resistance and a decrease in thermal conductivity.[47] Various surface functionalization, adopting covalent and non-covalent processes have been performed on BNNT to enhance its processability and promote compatibility with polymer matrices.[48−50] Defects and voids are inevitable on BNNT during covalent functionalization due to harsh modification conditions, while the intrinsic structure is preserved during non-covalent functionalization of BNNT due to mild modification conditions and, therefore, preferred over covalent modification.

Tannic acid (TA), a polyphenol derived from plants, consists of catechol and phenol in its structure. The binding affinity and surface adhesion of TA to various substrates have been demonstrated.[51] TA has been used to exfoliate and functionalize BN and BNNSs, resulting in enhanced thermal conductivity.[52,53] Furthermore, TA has significant potential for further reactions with other functional groups via oxidation. The presence of functional groups after non-covalent modifications of BNNT has been utilized to enhance their dispersion in polar and non-polar solvents and also in the polymer matrix.[45,54] The oxidized TA can form a quinone structure, which can then react with different moieties such as amine, thiol, and poly(acrylic acid).[55] These reactions can generate products having a strong binding affinity with the Al_2O_3 and epoxy polymer matrix.[56,57]

In this study, BNNT was deposited to protrude on the surface of Al_2O_3 to increase the contact points of fillers inside the epoxy matrix. For this, we propose a facile method to fabricate alkyl-functionalized BNNT using TA at very mild conditions. ODA was attached to the TA-coated BNNT to create functionalized BNNT (ODA-BNNT). ODA-BNNT was applied to the Al_2O_3 surface (Al_2O_3@ODA-BNNT) to form protruding BNNT on the surface of Al_2O_3. The protruding BNNT was exploited to increase the contact points of fillers to form a continuous network inside the epoxy matrix. The high-contact 3D network of fillers consequently enhanced heat dissipation and improved mechanical performance.

2. EXPERIMENTAL SECTION

2.1. Materials. TA and ethanol were obtained from Daejung Chemicals Co., Ltd., South Korea. Octadecylamine (ODA) was purchased from Tokyo Chemical Industries (TCI), Japan. Epoxy resin (171), hardener, and cross-linker (NADIC methyl anhydride; NMA) were supplied by Kukdo Chemicals Co., Ltd., South Korea. BNNT was obtained from Naieel Technology, South Korea. All utilized chemicals were used as is without any further purification. Deionized (DI) water was used to perform all of the experiments.

2.2. ODA-BNNT Preparation. For the amine functionalization of BNNT, TA (0.5, 1, 1.5, and 2%) was first dispersed into DI water (1000 mL) through bath sonication. Then, a fixed amount (1%) of BNNT was charged into the TA-containing beaker and bath sonicated for 10 min, followed by adjustment of pH 10 with NaOH (5%). Then, the setup was tip-sonicated for 60 min at an amplitude of 70% with a 15/02 on/off setting. After that, ODA (0.5, 1, 1.5, and 2%) was slowly added and tip-sonicated for 40 min. Finally, the product was recovered after repeated washing with water (5 times) and ethanol (5 times) each for 10 min using a centrifuge at 3000 rpm. Finally, the product was oven-dried at 70 °C for 10 h for subsequent composites formation.

2.3. Al_2O_3@ODA-BNNT Preparation. The surface-functionalized BNNT after oven-drying was used to deposit on the surface of Al_2O_3 (5 μm). The following technique was used to deposit ODA-BNNT on Al_2O_3. Ethanol (100 mL) was added into a beaker of a volume of 300 mL. To this end, different percentages (0.5, 1, 1.5, 2, and 2.5%) of ODA-BNNT were added. ODA-BNNT was dispersed into ethanol using bath sonication for 20 min. Then, 8 g of Al_2O_3 (5 μm) was added to the beaker and further bath sonicated for 10 min. Finally, the whole setup was moved to a hot plate to attach and protrude the ODA-BNNT on Al_2O_3 after evaporation of ethanol.

2.4. Epoxy Polymer Composites with Al_2O_3@ODA-BNNT. Different filler contents along with the ODA-BNNT were added to form epoxy composites to optimize the filler ratio (Table S1). Epoxy polymer composites were fabricated by mixing bisphenol A epoxy resin (171) and hardener (5:4 wt %) in a plastic container.[45] The prepared Al_2O_3@ODA-BNNT powder was added into the vessel containing polymer/

https://doi.org/10.1021/acsomega.4c05323
ACS Omega 2024, 9, 38946−38956

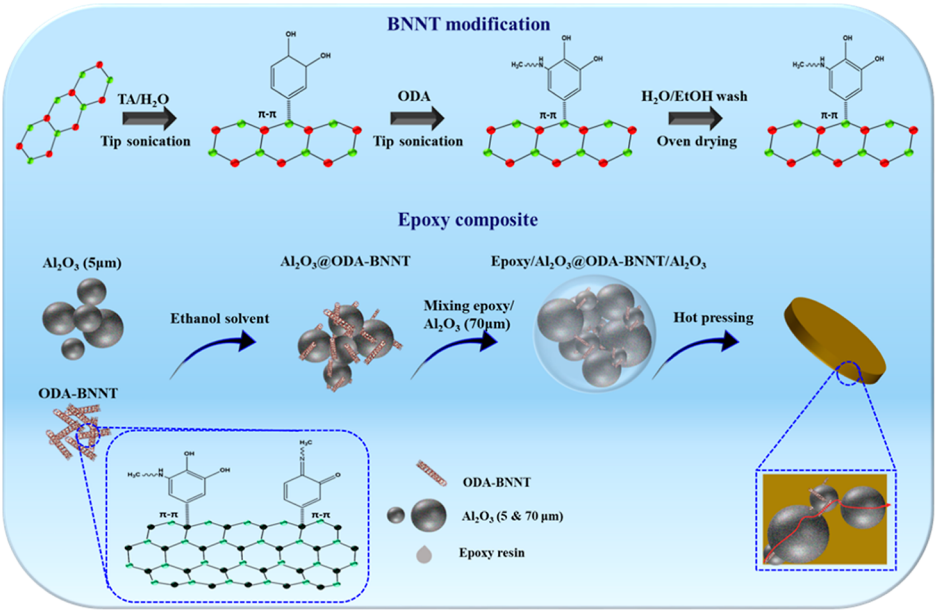

Figure 1. Schematic of BNNT modification and BNNT-deposited Al_2O_3 epoxy composite fabrication.

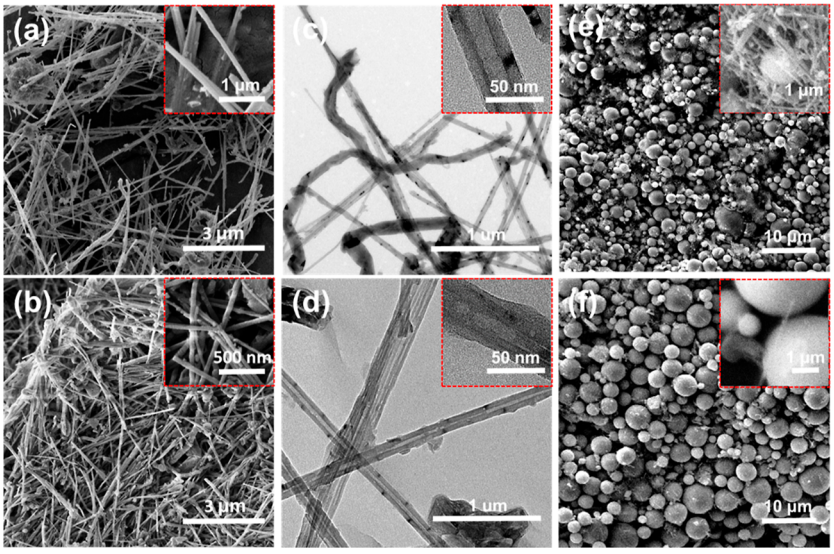

Figure 2. SEM images of (a,b) virgin BNNT and BNNT-ODA. (c,d) TEM images of virgin BNNT and BNNT-ODA SEM images (e,f) of Al_2O_3@ ODA-BNNT respectively.

hardener and a mechanical paste mix two times for 1 min each. Then, Al_2O_3 (70 μm) was added and was again paste mixed two times, 1 min each. Finally, NMA cross-linker was charged into it and paste mixed two times, 1 min each, to form the homogeneous composite pastes. The composite pastes were loaded in the steel mold to cure under pressure (120 °C for 1 h and at 150 °C for 3 h).[58] An identical process was used to prepare neat epoxy paste and virgin BNNT composite paste.

3. CHARACTERIZATIONS AND INSTRUMENTS

Scanning electron microscopy (SEM, CX-200 COXEM) combined with energy dispersive X-ray (EDX) was utilized to capture the microstructures of filler powder and epoxy composites. Detail surface analysis was performed using transmission electron microscopy (TEM; G2 F30 S-Twin; FEI, USA). Thermogravimetric analysis was performed to calculate the ODA on the surface of BNNT. For this, dried powder of all samples was loaded to TGA (Q500, TA Instruments, USA). Heating was applied from 50 to 900 °C at a rate of (10 °C/min). Crystallinity was observed using an X-ray diffractometer (XRD, PANalytical BV, the Netherlands). Differential scanning calorimetry (DSC) was measured by DSC4000 (PerkinElmer, Waltham, USA). Specific surface area (BET) was calculated using a Micromeritics ASAP 2420 (Micromeritics Instrument Corporation, Orcross, GA, USA). Thermal conduction was measured by a hot disk apparatus (Hot-Disk thermal analyzer, TPS500S, Sweden). For the analysis of the mechanical performance of all prepared samples, a universal testing machine (UMT, WITHLAB Co., Ltd., South Korea) was used. Thermal conductivity was measured at 25 °C, whereas the coefficient of thermal expansion (CTE) was performed at 0−190 °C, with a heating rate of 5 °C/min. Each analysis was conducted 5 times to obtain average values.

https://doi.org/10.1021/acsomega.4c05323
ACS Omega 2024, 9, 38946−38956

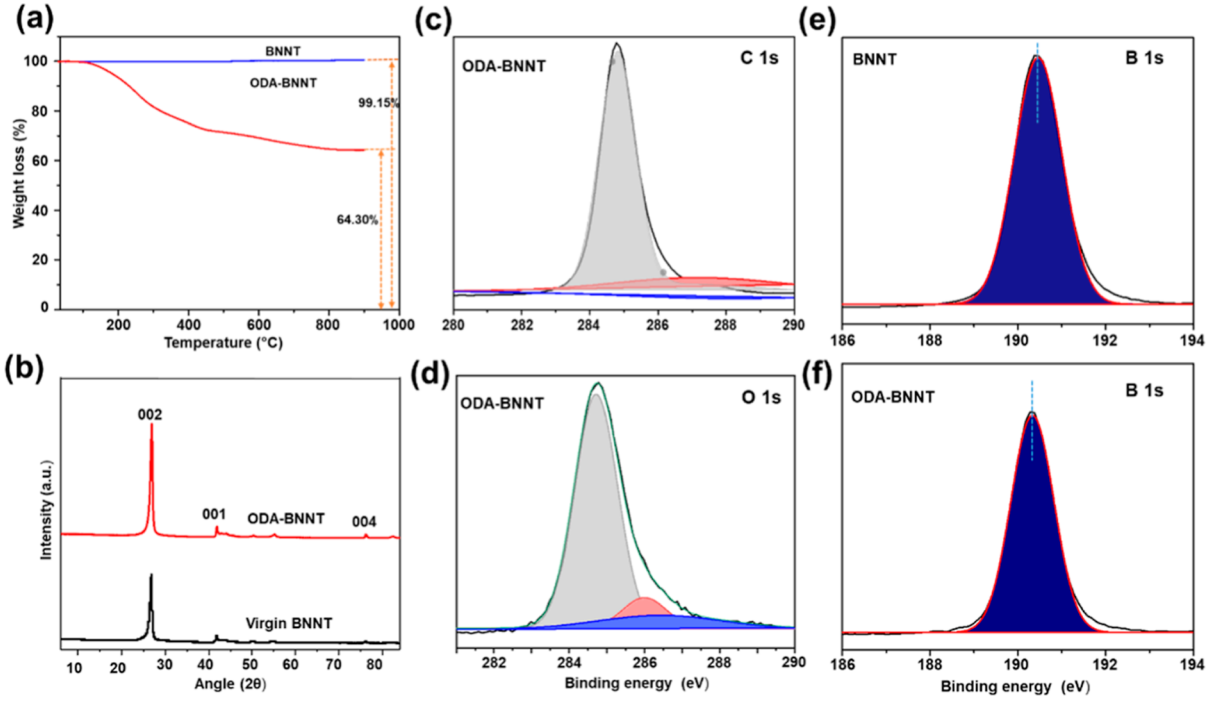

Figure 3. (a) TGA spectra, (b) XRD analysis, and (c–f) XPS spectra of virgin BNNT and ODA-BNNT.

4. RESULTS AND DISCUSSION

BNNT has been used as a filler to form high-performance thermally conductive composites to tackle thermal conduction issues. However, the presence of van der Waals interaction and entanglement in the virgin BNNT has a high tendency of agglomeration in the solvents and polymer matrix.[59] Moreover, the aggregated BNNT has a low potential to form a thermally conductive network to dissipate heat. However, a localized deposition strategy by depositing functionalized BNNT on the surface of Al_2O_3 is opted to solve the aforementioned issues.

Schematic diagram (Figure 1) shows the functionalization of BNNT and the fabrication process of the epoxy composites. A modified process was used to attach ODA to the surface of BNNT.[54] In the first step, TA was deposited on BNNT in an alkaline environment at pH 10, and it undergoes oxidation and oligomerization in an alkaline pH that increase its affinity to be deposited on BNNT.[54,60] The produced quinones, after the deposition of TA, were further reacted with amines of ODA through Michael addition to form ODA-BNNT.[61] The long alkyl chain-terminated BNNT can be well dispersed in ethanol to be deposited on the Al_2O_3 surface after the evaporation of ethanol. The formed ODA-BNNT was then deposited to protrude on the surface of Al_2O_3 by utilizing a solvent evaporation process. The formed Al_2O_3@ODA-BNNT in powder form was used to construct a continuous conduction network in the presence of a large-size Al_2O_3 (70 μm) filler. The SEM and TEM images of virgin BNNT and ODA-BNNT were captured to observe the surface morphology. SEM images of virgin and ODA-BNNT (Figure 2a,b) showed almost identical structures. A similar microstructure can be attributed to the finely localized nanodeposition of the ODA on the surface of the BNNT. TEM images (Figure 2c,d) displayed the structures of virgin and ODA-BNNT. A smooth surface structure of virgin BNNT was observed, having an average diameter of 30–50 nm, while a noticeable rough structure was observed in the ODA-BNNT due to the successful deposition of ODA on the surface of BNNT. Although a rough structure was observed after localized deposition of ODA but with a very thin coating of roughly ~8.3 nm thickness, the average diameter of BNNT nanotubes did not alter and remained identical after ODA deposition (Figure 2c,d). The SEM images of virgin BNNT and ODA-BNNT-deposited Al_2O_3 were also obtained to analyze the deposition trend of virgin BNNT and ODA-BNNT on the Al_2O_3 surface. Virgin BNNT, due to poor dispersion in the polymer matrix, formed aggregated deposition on Al_2O_3 (Figure 2e and inset). ODA-BNNT, however, due to the presence of long alkyl chains on the surface of BNNT, showed homogeneous distribution and firm attachment on the Al_2O_3 surface (Figure 2f and inset).[62]

The successful functionalization of BNNT with the attachment of an ODA is demonstrated by TGA and XPS analyses. The TGA spectra were obtained in an air environment to observe the deposited amount of ODA-BNNT (Figure 3a). The bulk BNNT showed almost the absence of any mass change up to 900 °C. The absence of mass loss is attributed to the excellent thermal stability and resistance to oxidation of BNNT.[63,64] ODA-BNNT, on the other hand, started to decompose above 200 °C due to the oxidation of aromatic moieties and the decomposition of carbonyl of TA.[65] Based on the weight retention fraction of virgin BNNT (99.15%) and the weight retention fraction of ODA-BNNT (64.30%), an amount of 34.85% of ODA was calculated to be deposited on the BNNT. The crystallinity analysis (XRD) was performed to observe the structures of virgin BNNT and ODA-BNNT (Figure 3b). The absence of any distinct features in both spectra demonstrated that BNNT, after modification, retains its inherent structure without any damage.

XPS wide spectra (Figure S2) and C 1s spectra of ODA-BNNT were obtained (Figure 3c), which revealed three peaks representing C═C, −C−O, and −C═O. The further O 1s spectra (Figure 3d) showed peaks of −O−C and −O−H that demonstrated the presence of TA-assisted ODA on the surface

https://doi.org/10.1021/acsomega.4c05323
ACS Omega 2024, 9, 38946−38956

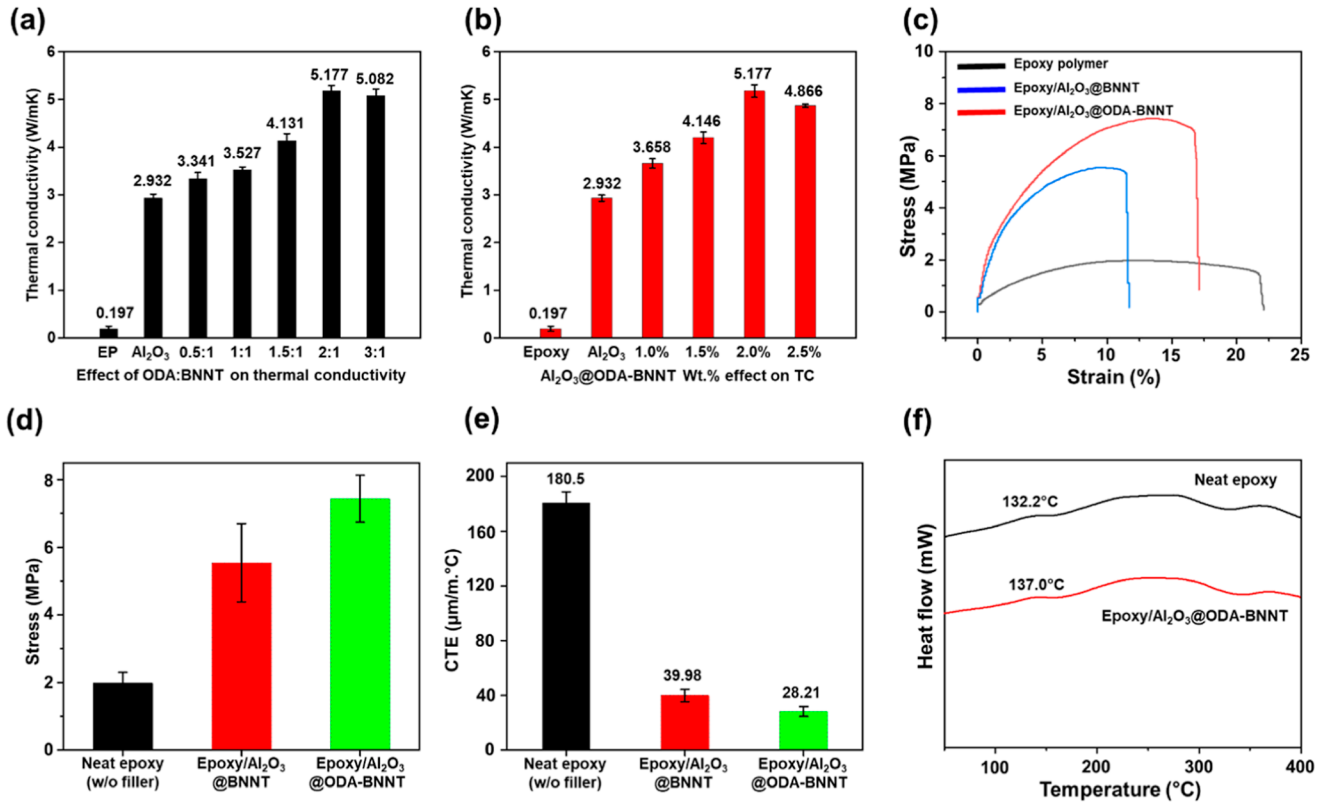

Figure 4. (a) Isotropic thermal conductivity of epoxy composites prepared with different ratios of ODA-BNNT, (b) with different wt % of Al_2O_3@ODA-BNNT, (c) tensile stress−strain curves, (d) tensile strength, and (e) CTE and (f) DSC curves and Al_2O_3@ODA-BNNT composite epoxy.

of BNNT, which is well matched to wide-range XPS (Figure S2). The wide-range XPS displayed more intense peaks of O 1s and C 1s for the ODA-BNNT than virgin BNNT that clearly demonstrated the attached TA-assisted ODA deposition on BNNT. ATR-FTIR (S3) further confirmed the deposited ODA on BNNT, compared to virgin BNNT, ODA-BNNT displayed sharp peaks at 29,280 and 2857 cm^{-1} corresponding to −C−H- symmetric and antisymmetric vibrations that represent CH_2 and CH_3 moieties of TA-attached ODA on BNNT, respectively.[47] Also, for B 1s (Figure 3e,f), the shifting of high binding energy implies the presence of TA due to the $\pi-\pi$ interaction between BNNT and the amine of the ODA. The specific surface area was calculated for both virgin and modified BNNT. A specific surface area of 53.249 ± 0.4104 m^2/g was analyzed for virgin BNNT, whereas 54.361 ± 0.331 m^2/g was found for ODA-BNNT. The enhanced surface area can be attributed to the localized deposited ODA on the BNNT surface.

The 1D structural features of BNNT enable it to display excellent thermal conductivity while resisting thermal oxidation.[63] BNNT, like other 1D fillers, has interaction with various fillers such as Al_2O_3 and AlN to increase the thermal conductivity by forming thermal conduction paths.[66] However, due to poor interaction and the absence of any bonding between Al_2O_3 and the co-filler, there is a high probability that the 1D filler could lose contact with the main filler to interact with the polymer matrix, which could subsequently reduce processability. ODA-BNNT, however, due to its binding ability on the surface of Al_2O_3, can be a potential strategy to strongly intact the individual BNNT on the surface of Al_2O_3. The attached ODA-BNNT will not only interact with the Al_2O_3 filler to increase thermal conduction but will also be entangled with the polymer matrix to enhance the mechanical performance of composites.

For this, ODA-BNNT, after optimization of all parameters, was utilized to prepare composite samples with epoxy resin (Figure 4a,b). Different parameters, including TA, ODA concentrations, and wt % addition, were analyzed as follows: first, different concentration ratios (0.5:1, 1:1, 1.5:1, and 2:1) of TA: BNNT were used to optimize TA concentrations (Figure S5). A 1:1 ratio was collected to be an optimized ratio. When increasing the amount of TA (TA:BNNT; 1.5:1 and 2:1), a lower thermal conduction was observed. The lower thermal conduction can be ascribed to the poor dispersion of BNNT when containing a higher amount of TA. The higher amount of TA on the surface of BNNT (more than optimized 1:1) may cause strong binding to form aggregation among the BNNT, consequently lowering their dispersion in the polymer matrix. After that, the ODA concentration ratio was optimized against prepared TA-deposited BNNT (Figure S6). Different ratios (0.5:1, 1:1, 1.5:1.5, 2:1, and 3:1) of the ODA:TA-BNNT were used to collect the optimized concentration to fabricate epoxy composites (Figure 4a). A 2:1 ratio was selected as an optimized ratio based on the enhancement of thermal conduction. By further increasing the ODA amount (3:1), an absence of thermal conduction improvement was observed. The absence of enhancement may be attributed to the amount of deposited TA on the BNNT surface. When further increasing the ODA ratio (3:1), the excess ODA was unable to be deposited on the TA-BNNT; hence, the excess ODA can be removed during centrifugation/washing with ethanol. Therefore, an optimized ratio of 2:1 was set to prepare epoxy composites to analyze various characteristics, including

https://doi.org/10.1021/acsomega.4c05323
ACS Omega 2024, 9, 38946−38956

mechanical performance, heating/cooling cycles, and CTE (Figure S4).

An optimized ratio of 2:1 of ODA-BNNT was obtained to display the highest thermal conductivity when added 2 wt % to the composite. By further increasing the wt % of ODA-BNNT (2.5 wt %) to the epoxy matrix, however, a decrease in thermal conduction was observed. As the loading of the ODA-BNNT filler exceeds the threshold percolation level (>2 wt %), aggregation may start because of poor dispersion of ODA-BNNT into the epoxy matrix at higher concentrations, which eventually reduces the thermal conduction of composites.[67]

The mechanical performance of epoxy composites is also an important factor, in addition to thermal conduction, for their effective application. The tensile strength performance of epoxy composites with Al_2O_3@BNNT and Al_2O_3@ODA-BNNT was studied (Figure 4c). The tensile strength of epoxy with Al_2O_3@BNNT and with Al_2O_3@ODA-BNNT was reached at 5.54 and 7.43 MPa, respectively (Figure 4d). The incorporation of both Al_2O_3@BNNT and Al_2O_3@ODA-BNNT significantly enhanced the mechanical performance due to the unique tube-like structure of BNNT. The subsequent enhancement can be associated with the 1D structural features, dispersion effectiveness, and ODA compatibility with the polymer matrix.[68] The better performance of Al_2O_3@ODA-BNNT, however, suggested that the surface functionalization not only increased the thermal conductivity due to the strong attachment of ODA-BNNT with Al_2O_3 that promotes the formation of a thermal conduction network to dissipate the generated heat but also prevented the formation of stress concentrations due to the even distribution and improved interfacial adhesion of ODA-BNNT with the epoxy matrix.[62,69,70] Well-distribution of ODA-BNNT into the epoxy matrix induces strength by transferring the stress from the epoxy matrix to the ODA-BNNT nanofillers.[71]

A low CTE and excellent thermal stability are vital for the utilization of polymer composites. Low CTE is highly demanded when high-temperature flux is encountered in different application areas, including aerospace, composite coatings, and thermal conduction materials. Numerous fillers have been used to fabricate polymer composites with low CTE.[72,73] Various factors, such as volume fraction, aspect ratio, and orientation of fillers, have been involved in effecting the CTE of composites.[74] The CTE of the prepared epoxy composites in the presence of Al_2O_3@BNNT and Al_2O_3@ODA-BNNT was compared with that of neat epoxy polymer (Figure 4e). A high CTE of 180.5 ± 8.256 μm/m °C was obtained for the neat epoxy sample. However, a drastic reduction in CTE was observed when virgin BNNT and modified BNNT in the form of Al_2O_3@BNNT and Al_2O_3@ODA-BNNT were introduced in the polymer matrix. Lower CTE values of 39.98 ± 4.481 and 28.21 ± 3.642 μm/m °C were recorded when virgin and modified BNNT were included in the polymer matrix. The reduced CTE values can be attributed to the 1D structural features of modified BNNT that render their homogeneous distribution into the polymer matrix along with strong interactions with the epoxy resin. Glass transition temperature (T_g) is considered an important parameter to compare the thermal behavior of the composites. Since the intermediate temperature is denoted as T_g, neat epoxy displayed T_g at 132.2 °C, whereas the T_g of Al_2O_3@ODA-BNNT containing epoxy was observed at 137 °C. The shifting of T_g toward higher temperatures can be explained by the fact that the increase of T_g with the addition of fillers reduced the mobility of epoxy chains. The presence of fillers can act as a physical interlocking point that restrains the chain mobility.[71] Also, the presence of long alkyl chains on modified BNNT can be entangled with the epoxy matrix to increase the T_g of composites.[75]

Microstructures were collected using SEM images to evaluate the distribution and dispersion of Al_2O_3@ODA-BNNT into the epoxy matrix (Figure 5a–d). An improved

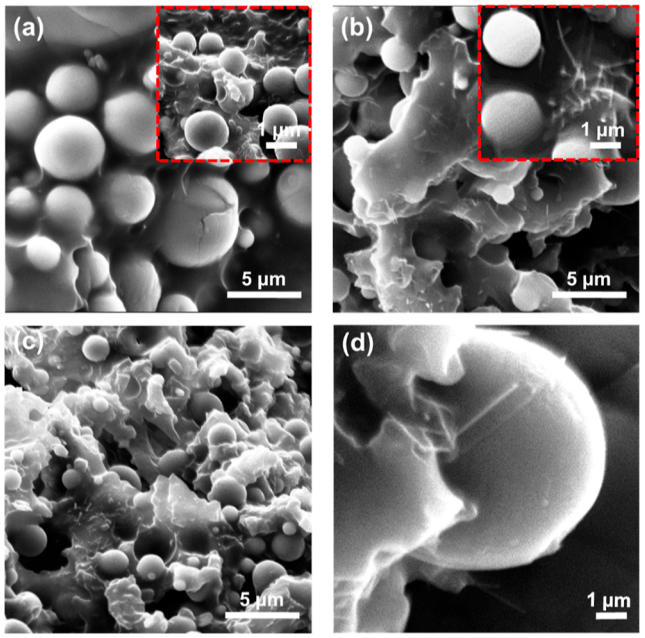

Figure 5. SEM images of composites prepared with epoxy (a) without BNNT, (b) with Al_2O_3@BNNT, (c) with Al_2O_3@ODA-BNNT, and (d) magnified image of Al_2O_3@ODA-BNNT.

thermal conductivity, mechanical strength, and lower values of CTE were observed when compared to those without BNNT, virgin BNNT (Al_2O_3@BNNT) and modified BNNT (Al_2O_3@ODA-BNNT) were used. The microstructure of composite without BNNT showed gaps between the Al_2O_3 particles to allow the heat flow less efficiently (Figure 5a and inset). An aggregated BNNT was observed in the matrix when virgin BNNT was used to attach to the Al_2O_3 surface (Figure 5b and the inset). Modified BNNT in the form of Al_2O_3@ODA-BNNT, however, displayed a homogeneous distribution of BNNT attached to the surface of Al_2O_3 (Figure 5c). It is worth noticing that the strong adhesion of ODA-BNNT to Al_2O_3 is highly retained even after compounding with epoxy resin (Figure 5d). The robust attached BNNT can be attributed to the TA-assisted ODA modification that enabled BNNT to be attached to the surface of Al_2O_3 and subsequently evenly distributed into the whole epoxy matrix to enhance the mechanical properties of epoxy composites.

Infrared (IR) thermal images were captured during the heating and cooling cycles for a particular time of 150 and 250 s, respectively (Figure 6a). The obtained IR images showed improved heating of the composites in the presence of both virgin and modified BNNT in the form of Al_2O_3@BNNT and Al_2O_3@ODA-BNNT, respectively. A swift thermal response was recorded in the presence of Al_2O_3@ODA-BNNT. The improved thermal response (fast absorption and release of heat) demonstrates the formation of improved thermal

https://doi.org/10.1021/acsomega.4c05323
ACS Omega 2024, 9, 38946−38956

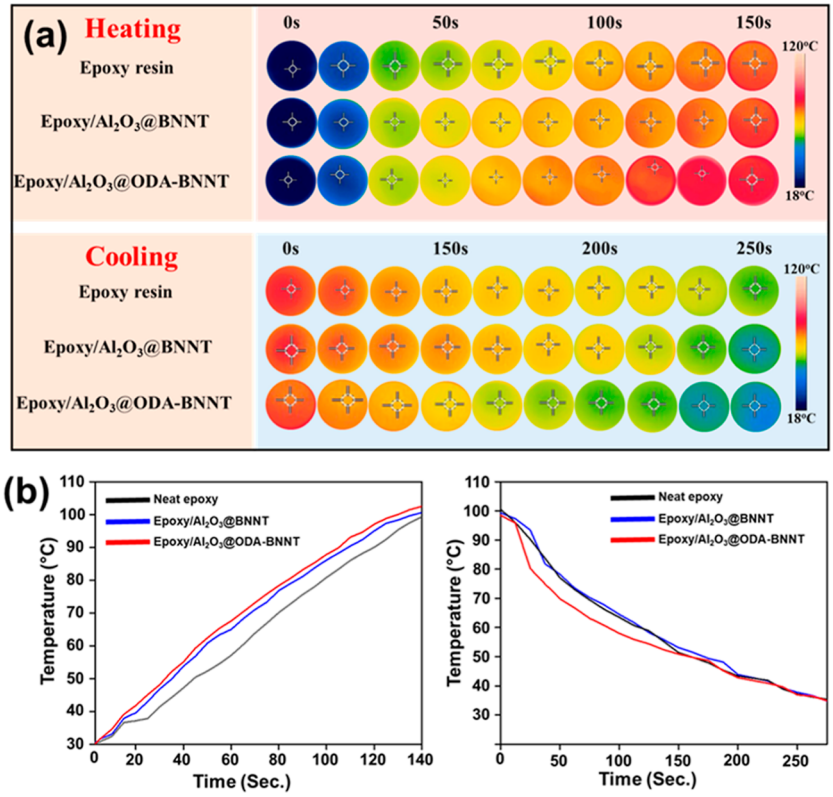

Figure 6. (a) Infrared images of neat epoxy, epoxy with Al_2O_3@BNNT, and epoxy with Al_2O_3@ODA-BNNT during heating and cooling cycles. (b) Temperature variations against time during heating/cooling cycles.

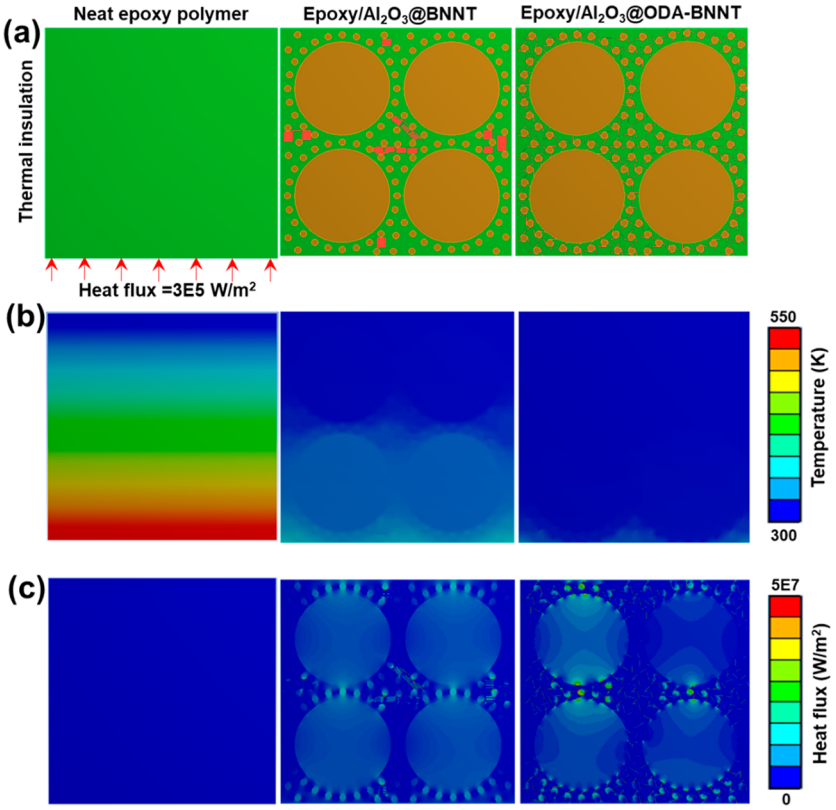

Figure 7. (a) Boundary conditions of neat epoxy (left), Al_2O_3@BNNT filler epoxy (center), and Al_2O_3@ODA-BNNT (right)-filled epoxy, respectively. (b) Heat flux of all samples and (c) heat flow inside the matrix of samples.

https://doi.org/10.1021/acsomega.4c05323
ACS Omega 2024, 9, 38946−38956

conduction pathways to dissipate heat more effectively than neat epoxy and virgin BNNT (Figure 6b).[76]

The insight into the conduction pathways was further collected using finite element analysis and an ANSYS simulation. Three different models were applied, including a neat epoxy matrix, an epoxy matrix containing Al_2O_3@BNNT, and Al_2O_3@ODA-BNNT-filled epoxy composites. The utilized models were set with identical boundary conditions, i.e., convection at the top with a free air stream of 300 K, both sides were insulated, and the bottom part was set as a heat flux of 3ES W/m^2 (Figure 7a). The simulation calculation is based on the steady-state heat transfer based on two equations[77,78]

$$\nabla \cdot \vec{q} = Q \tag{1}$$

$$\vec{q} = -k\nabla T \tag{2}$$

where $\vec{q}$ is the heat flux vector that presents the flow of heat per unit area per unit time, Q is the heat generation inside the material matrix, such as heat from chemical reactions ($Q = 0$ in this study), T is the temperature, ∇ is a vector differential operator, and k is the thermal conductivity of materials. Thermal conductivity values of 0.2, 30, and 300 W/mK were set for neat epoxy and composites in the presence of Al2O3@BNNT and Al2O3@ODA-BNNT, respectively.[63]

The addition of fillers, Al_2O_3@BNNT and Al_2O_3@ODA-BNNT, significantly increases the heat transfer in the polymer matrix when compared with neat epoxy polymer (Figure 7b,c). When neat BNNT was used to attach to the surface of Al_2O_3, an uneven distribution resulted due to the aggregation of virgin BNNT. In contrast, ODA-BNNT-attached Al_2O_3, however, displayed an even distribution of BNNT into the entire epoxy matrix to form thermal conduction pathways to effectively dissipate the heat during TMM applications.

Table S2 summarizes some recent research results on thermal conduction and mechanical performance with different polymer matrices and filler systems. Based on the results, a small fraction of modified BNNT (0.5−2 wt %) can significantly enhance thermal and mechanical performance by facilitating improved contact points among the Al_2O_3 filler.[79] Moreover, the devised modification of the BNNT is simple and straightforward and can scale up easily.

5. CONCLUSIONS

In summary, this study outlines a successful approach for achieving a uniform distribution of BNNT within the epoxy matrix. A TA-assisted amine-modified BNNT is firmly bonded to the surface of Al_2O_3, generating a heat transfer network. The epoxy/Al_2O_3@ODA-BNNT composite demonstrates improved properties, such as enhanced mechanical performance and high thermal conduction. The optimized filler content enhances the thermal conductivity while preserving excellent mechanical performance. The improved performance is credited to the uniform dispersion of the modified BNNT, which creates a seamless network throughout the matrix, thus enhancing thermal conduction. In addition, the BNNT modified with alkyl chains exhibited a significant interaction with the epoxy matrix, resulting in improved mechanical performance. The study offers a practical approach to producing epoxy composites on a larger scale, which can effectively address heat dissipation challenges in industries such as batteries and electric vehicles.

ASSOCIATED CONTENT

Supporting Information

The Supporting Information is available free of charge at https://pubs.acs.org/doi/10.1021/acsomega.4c05323.

EDX mapping of ODA-BNNT prepared using 2:1, XPS wide spectra and element analysis of neat BNNT and ODA-BNNT, FT-IR spectra of neat BNNT and modified BNNT in the form of ODA-BNNT, EDX of the ODA-BNNT/Al_2O_3 epoxy composite, table of filler type and filler composition in the epoxy matrix, thermal conductivity of TA-BNNT deposited on Al_2O_3 epoxy composites, thermal conductivity of epoxy composites with different wt % of TA-BNNT, and thermal conductivity and tensile stress performance of different polymer/filler composites (PDF)

AUTHOR INFORMATION

Corresponding Author

Jaewoo Kim − *R&D Center, Naieel Technology, Daejeon 34104, Republic of Korea;* orcid.org/0000-0003-3472-0180; Phone: +82427163012; Email: kimj@naieel.com

Authors

Zahid Hanif − *R&D Center, Naieel Technology, Daejeon 34104, Republic of Korea*

Duy Khoe Dinh − *R&D Center, Naieel Technology, Daejeon 34104, Republic of Korea*

Arni Gesselle M. Pornea − *R&D Center, Naieel Technology, Daejeon 34104, Republic of Korea;* orcid.org/0000-0002-3357-3257

Numan Yanar − *R&D Center, Naieel Technology, Daejeon 34104, Republic of Korea*

Min Seok Kwak − *CMT Co., Ltd., Seoul 06211, Republic of Korea*

Complete contact information is available at: https://pubs.acs.org/10.1021/acsomega.4c05323

Notes

The authors declare no competing financial interest.

ACKNOWLEDGMENTS

This work was financially supported by the Scale-Up TIPS R&D Projects Grant no. RS-2023-00285159 sponsored by the Ministry of SMEs and Startups and Grant no. 20017989 (ATC + Program) sponsored by the Ministry of Trade, Industry, and Energy of the Republic of Korea.

REFERENCES

(1) Lin, C.-H.; Fu, H.-C.; Cheng, B.; Tsai, M.-L.; Luo, W.; Zhou, L.; Jang, S.-H.; Hu, L.; He, J.-H. A flexible solar-blind 2D boron nitride nanopaper-based photodetector with high thermal resistance. *npj 2D Mater. Appl.* **2018**, *2* (1), 23.

(2) Feng, C.-P.; Chen, L.-B.; Tian, G.-L.; Wan, S.-S.; Bai, L.; Bao, R.-Y.; Liu, Z.-Y.; Yang, M.-B.; Yang, W. Multifunctional thermal management materials with excellent heat dissipation and generation capability for future electronics. *ACS Appl. Mater. Interfaces* **2019**, *11* (20), 18739−18745.

(3) Niu, H.; Ren, Y.; Guo, H.; Małycha, K.; Orzechowski, K.; Bai, S.-L. Recent progress on thermally conductive and electrical insulating rubber composites: Design, processing and applications. *Compos. Commun.* **2020**, *22*, 100430.

(4) Guo, Y.; Ruan, K.; Shi, X.; Yang, X.; Gu, J. Factors affecting thermal conductivities of the polymers and polymer composites: A review. *Compos. Sci. Technol.* **2020**, *193*, 108134.
(5) Chen, J.; Huang, X.; Zhu, Y.; Jiang, P. Cellulose nanofiber supported 3D interconnected BN nanosheets for epoxy nanocomposites with ultrahigh thermal management capability. *Adv. Funct. Mater.* **2017**, *27* (5), 1604754.
(6) Wu, Y.; Xue, Y.; Qin, S.; Liu, D.; Wang, X.; Hu, X.; Li, J.; Wang, X.; Bando, Y.; Golberg, D.; et al. BN nanosheet/polymer films with highly anisotropic thermal conductivity for thermal management applications. *ACS Appl. Mater. Interfaces* **2017**, *9* (49), 43163−43170.
(7) Huang, X.; Ma, S.; Zhao, C.; Wang, H.; Ju, S. Exploring high thermal conductivity polymers via interpretable machine learning with physical descriptors. *npj Comput. Mater.* **2023**, *9* (1), 191.
(8) Do, N. B. D.; Imenes, K.; Aasmundtveit, K. E.; Nguyen, H.-V.; Andreassen, E. Thermal Conductivity and Mechanical Properties of Polymer Composites with Hexagonal Boron Nitride—A Comparison of Three Processing Methods: Injection Moulding, Powder Bed Fusion and Casting. *Polymers* **2023**, *15* (6), 1552.
(9) Hu, Q.; Bai, X.; Zhang, C.; Zeng, X.; Huang, Z.; Li, J.; Li, J.; Zhang, Y. Oriented BN/Silicone rubber composite thermal interface materials with high out-of-plane thermal conductivity and flexibility. *Composites, Part A* **2022**, *152*, 106681.
(10) Yan, Z.; Cai, X.; Liang, H.; Tang, J.; Gou, Q.; Wang, W.; Gao, Y.; Qin, M.; Tan, H.; Cai, J. Thermally Conductive Epoxy Resin Composites Based on 3D Graphene Nanosheet Networks for Electronic Package Heat Dissipation. *ACS Appl. Nano Mater.* **2024**, *7*, 12644−12652.
(11) Li, J.; Liu, X.; Feng, Y.; Yin, J. Recent progress in polymer/two-dimensional nanosheets composites with novel performances. *Prog. Polym. Sci.* **2022**, *126*, 101505.
(12) Chen, Q.; Ma, Z.; Wang, M.; Wang, Z.; Feng, J.; Chevali, V.; Song, P. Recent advances in nacre-inspired anisotropic thermally conductive polymeric nanocomposites. *Nano Res.* **2023**, *16* (1), 1362−1386.
(13) Hao, L.; Chen, J.; Ma, T.; Cheng, J.; Zhang, J.; Zhao, F. Low dielectric and high performance of epoxy polymer via grafting POSS dangling chains. *Eur. Polym. J.* **2022**, *173*, 111313.
(14) Madsen, F. B.; Daugaard, A. E.; Hvilsted, S.; Skov, A. L. The current state of silicone-based dielectric elastomer transducers. *Macromol. Rapid Commun.* **2016**, *37* (5), 378−413.
(15) Zha, J.-W.; Zhu, Y.-H.; Li, W.-K.; Bai, J.; Dang, Z.-M. Low dielectric permittivity and high thermal conductivity silicone rubber composites with micro-nano-sized particles. *Appl. Phys. Lett.* **2012**, *101* (6), 062905.
(16) Zhang, L.; Wang, D.; Hu, P.; Zha, J.-W.; You, F.; Li, S.-T.; Dang, Z.-M. Highly improved electro-actuation of dielectric elastomers by molecular grafting of azobenzenes to silicon rubber. *J. Mater. Chem. C* **2015**, *3* (19), 4883−4889.
(17) Singh, V.; Bougher, T. L.; Weathers, A.; Cai, Y.; Bi, K.; Pettes, M. T.; McMenamin, S. A.; Lv, W.; Resler, D. P.; Gattuso, T. R.; et al. High thermal conductivity of chain-oriented amorphous polythiophene. *Nat. Nanotechnol.* **2014**, *9* (5), 384−390.
(18) Song, N.; Cao, D.; Luo, X.; Wang, Q.; Ding, P.; Shi, L. Highly thermally conductive polypropylene/graphene composites for thermal management. *Composites, Part A* **2020**, *135*, 105912.
(19) Li, Y.-T.; Liu, W.-J.; Shen, F.-X.; Zhang, G.-D.; Gong, L.-X.; Zhao, L.; Song, P.; Gao, J.-F.; Tang, L.-C. Processing, thermal conductivity and flame retardant properties of silicone rubber filled with different geometries of thermally conductive fillers: A comparative study. *Composites, Part B* **2022**, *238*, 109907.
(20) Jiang, F.; Cui, X.; Song, N.; Shi, L.; Ding, P. Synergistic effect of functionalized graphene/boron nitride on the thermal conductivity of polystyrene composites. *Compos. Commun.* **2020**, *20*, 100350.
(21) Lv, X.; Tang, Y.; Tian, Q.; Wang, Y.; Ding, T. Ultra-stretchable membrane with high electrical and thermal conductivity via electrospinning and in-situ nanosilver deposition. *Compos. Sci. Technol.* **2020**, *200*, 108414.
(22) Wang, H.; Yang, H.; Wang, Q.; Tong, J.; Wen, J.; Zhang, Q. Surface-modified Li3Mg2NbO6 ceramic particles and hexagonal boron nitride sheets filled PTFE composites with high through-plane thermal conductivity and extremely low dielectric loss. *Compos. Commun.* **2020**, *22*, 100523.
(23) Oh, H.; Kim, Y.; Wie, J.; Kim, K.; Kim, J. Tailoring of Si−C−N−O ceramic-coated reduced graphene oxide by oil/water-solution process for high thermal conductive epoxy composite with electrical insulation. *Compos. Sci. Technol.* **2020**, *197*, 108257.
(24) Chen, Q.; Liu, L.; Zhang, A.; Wang, W.; Wang, Z.; Zhang, J.; Feng, J.; Huo, S.; Zeng, X.; Song, P. An iron phenylphosphinate@graphene oxide nanohybrid enabled flame-retardant, mechanically reinforced, and thermally conductive epoxy nanocomposites. *Chem. Eng. J.* **2023**, *454*, 140424.
(25) Chen, Q.; Huo, S.; Lu, Y.; Ding, M.; Feng, J.; Huang, G.; Xu, H.; Sun, Z.; Wang, Z.; Song, P. Heterostructured Graphene@ Silica@ Iron Phenylphosphinate for Fire-Retardant, Strong, Thermally Conductive Yet Electrically Insulated Epoxy Nanocomposites. *Small* **2024**, *20*, 2310724.
(26) Chen, Q.; Ma, Z.; Wang, Z.; Liu, L.; Zhu, M.; Lei, W.; Song, P. Scalable, robust, low-cost, and highly thermally conductive anisotropic nanocomposite films for safe and efficient thermal management. *Adv. Funct. Mater.* **2022**, *32* (8), 2110782.
(27) Wieme, T.; Duan, L.; Mys, N.; Cardon, L.; D'hooge, D. R. Effect of matrix and graphite filler on thermal conductivity of industrially feasible injection molded thermoplastic composites. *Polymers* **2019**, *11* (1), 87.
(28) Shen, H.; Guo, J.; Wang, H.; Zhao, N.; Xu, J. Bioinspired modification of h-BN for high thermal conductive composite films with aligned structure. *ACS Appl. Mater. Interfaces* **2015**, *7* (10), 5701−5708.
(29) Wang, J.; Liu, D.; Li, Q.; Chen, C.; Chen, Z.; Song, P.; Hao, J.; Li, Y.; Fakhrhoseini, S.; Naebe, M.; et al. Lightweight, superelastic yet thermoconductive boron nitride nanocomposite aerogel for thermal energy regulation. *ACS Nano* **2019**, *13* (7), 7860−7870.
(30) Chen, Q.; Wang, Z. A copper organic phosphonate functionalizing boron nitride nanosheet for PVA film with excellent flame retardancy and improved thermal conductive property. *Composites, Part A* **2022**, *153*, 106738.
(31) Ramdani, N.; Derradji, M.; Feng, T.-t.; Tong, Z.; Wang, J.; Mokhnache, E.-O.; Liu, W.-b. Preparation and characterization of thermally-conductive silane-treated silicon nitride filled polybenzoxazine nanocomposites. *Mater. Lett.* **2015**, *155*, 34−37.
(32) Wei, Z.; Xie, W.; Ge, B.; Zhang, Z.; Yang, W.; Xia, H.; Wang, B.; Jin, H.; Gao, N.; Shi, Z. Enhanced thermal conductivity of epoxy composites by constructing aluminum nitride honeycomb reinforcements. *Compos. Sci. Technol.* **2020**, *199*, 108304.
(33) Moreira, D.; Braga Junior, N.; Benevides, R.; Sphaier, L.; Nunes, L. Temperature-dependent thermal conductivity of silicone-Al_2O_3 nanocomposites. *Appl. Phys. A: Mater. Sci. Process.* **2015**, *121*, 1227−1234.
(34) Song, P.; Wang, C.; Chen, L.; Zheng, Y.; Liu, L.; Wu, Q.; Huang, G.; Yu, Y.; Wang, H. Thermally stable, conductive and flame-retardant nylon 612 composites created by adding two-dimensional alumina platelets. *Composites, Part A* **2017**, *97*, 100−110.
(35) Song, J.; Peng, Z.; Zhang, Y. Enhancement of thermal conductivity and mechanical properties of silicone rubber composites by using acrylate grafted siloxane copolymers. *Chem. Eng. J.* **2020**, *391*, 123476.
(36) Wu, Y.; Ye, K.; Liu, Z.; Wang, B.; Yan, C.; Wang, Z.; Lin, C.-T.; Jiang, N.; Yu, J. Cotton candy-templated fabrication of three-dimensional ceramic pathway within polymer composite for enhanced thermal conductivity. *ACS Appl. Mater. Interfaces* **2019**, *11* (47), 44700−44707.
(37) Niu, H.; Guo, H.; Ren, Y.; Ren, L.; Lv, R.; Kang, L.; Bashir, A.; Bai, S. Spherical aggregated BN/AlN filled silicone composites with enhanced through-plane thermal conductivity assisted by vortex flow. *Chem. Eng. J.* **2022**, *430*, 133155.

https://doi.org/10.1021/acsomega.4c05323
ACS Omega 2024, 9, 38946−38956

(38) Deeksha, B.; Sadanand, V.; Hariram, N.; Rajulu, A. V. Preparation and properties of cellulose nanocomposite fabrics with in situ generated silver nanoparticles by bioreduction method. *J. Bioresour. Bioprod.* **2021**, *6* (1), 75−81.
(39) Im, H.; Kim, J. The effect of Al_2O_3 doped multi-walled carbon nanotubes on the thermal conductivity of Al_2O_3/epoxy terminated poly (dimethylsiloxane) composites. *Carbon* **2011**, *49* (11), 3503−3511.
(40) Kim, Y.-K.; Chung, J.-Y.; Lee, J.-G.; Baek, Y.-K.; Shin, P.-W. Synergistic effect of spherical Al_2O_3 particles and BN nanoplates on the thermal transport properties of polymer composites. *Composites, Part A* **2017**, *98*, 184−191.
(41) Lu, Y.; Zhao, R.; Wang, L.; Songfeng, E. Boron nitride nanotubes and nanosheets: Their basic properties, synthesis, and some of applications. *Diamond Relat. Mater.* **2023**, *136*, 109978.
(42) Jiang, X.-F.; Weng, Q.; Wang, X.-B.; Li, X.; Zhang, J.; Golberg, D.; Bando, Y. Recent progress on fabrications and applications of boron nitride nanomaterials: a review. *J. Mater. Sci. Technol.* **2015**, *31* (6), 589−598.
(43) Smith, K. K.; Redeker, N. D.; Rios, J. C.; Mecklenburg, M. H.; Marcischak, J. C.; Guenthner, A. J.; Ghiassi, K. B. Surface modification and functionalization of boron nitride nanotubes via condensation with saturated and unsaturated alcohols for high performance polymer composites. *ACS Appl. Nano Mater.* **2019**, *2* (7), 4053−4060.
(44) Mohanraman, R.; Steiner, P.; Kocabas, C.; Kinloch, I. A.; Bissett, M. A. Synergistic Improvement in the Thermal Conductivity of Hybrid Boron Nitride Nanotube/Nanosheet Epoxy Composites. *ACS Appl. Nano Mater.* **2024**, *7*, 13142−13146.
(45) Hanif, Z.; Khoe, D. D.; Choi, K.-I.; Jung, J.-H.; Pornea, A. G. M.; Yanar, N.; Kwak, C.; Kim, J. Synergistic effect on dispersion, thermal conductivity and mechanical performance of pyrene modified boron nitride nanotubes with Al_2O_3/epoxy composites. *Compos. Sci. Technol.* **2024**, *247*, 110419.
(46) Liang, L.; Hu, W.; Zhang, Z.; Shen, J.-W. Theoretic study on dispersion mechanism of boron nitride nanotubes by polynucleotides. *Sci. Rep.* **2016**, *6* (1), 39747.
(47) Yu, L.; Gao, S.; Yang, D.; Wei, Q.; Zhang, L. Improved thermal conductivity of polymer composites by noncovalent modification of boron nitride via tannic acid chemistry. *Ind. Eng. Chem. Res.* **2021**, *60* (34), 12570−12578.
(48) de los Reyes, C. A.; Walz Mitra, K. L.; Smith, A. D.; Yazdi, S.; Loredo, A.; Frankovsky, F. J.; Ringe, E.; Pasquali, M.; Martí, A. A. Chemical decoration of boron nitride nanotubes using the Billups-Birch reaction: toward enhanced thermostable reinforced polymer and ceramic nanocomposites. *ACS Appl. Nano Mater.* **2018**, *1* (5), 2421−2429.
(49) Kim, D.; Nakajima, S.; Sawada, T.; Iwasaki, M.; Kawauchi, S.; Zhi, C.; Bando, Y.; Golberg, D.; Serizawa, T. Sonication-assisted alcoholysis of boron nitride nanotubes for their sidewalls chemical peeling. *Chem. Commun.* **2015**, *51* (33), 7104−7107.
(50) Shin, H.; Guan, J.; Zgierski, M. Z.; Kim, K. S.; Kingston, C. T.; Simard, B. Covalent functionalization of boron nitride nanotubes via reduction chemistry. *ACS Nano* **2015**, *9* (12), 12573−12582.
(51) Liu, L.; Shi, H.; Yu, H.; Zhou, R.; Yin, J.; Luan, S. One-step hydrophobization of tannic acid for antibacterial coating on catheters to prevent catheter-associated infections. *Biomater. Sci.* **2019**, *7* (12), 5035−5043.
(52) Wu, N.; Yang, W.; Che, S.; Sun, L.; Li, H.; Ma, G.; Sun, Y.; Liu, H.; Wang, X.; Li, Y. Green preparation of high-yield and large-size hydrophilic boron nitride nanosheets by tannic acid-assisted aqueous ball milling for thermal management. *Composites, Part A* **2023**, *164*, 107266.
(53) Zhao, L.; Yan, L.; Wei, C.; Wang, Z.; Jia, L.; Ran, Q.; Huang, X.; Ren, J. Aqueous-phase exfoliation and functionalization of boron nitride nanosheets using tannic acid for thermal management applications. *Ind. Eng. Chem. Res.* **2020**, *59* (37), 16273−16282.
(54) Hanif, Z.; Choi, K.-I.; Jung, J.-H.; Pornea, A. G. M.; Park, E.; Cha, J.; Kim, H.-R.; Choi, J.-H.; Kim, J. Dispersion enhancement of boron nitride nanotubes in a wide range of solvents using plant polyphenol-based surface modification. *Ind. Eng. Chem. Res.* **2023**, *62* (6), 2662−2670.
(55) Chen, C.; Yang, H.; Yang, X.; Ma, Q. Tannic acid: A crosslinker leading to versatile functional polymeric networks: A review. *RSC Adv.* **2022**, *12* (13), 7689−7711.
(56) Xu, L. Q.; Neoh, K.-G.; Kang, E.-T. Natural polyphenols as versatile platforms for material engineering and surface functionalization. *Prog. Polym. Sci.* **2018**, *87*, 165−196.
(57) Xu, R.; Ma, S.; Lin, P.; Yu, B.; Zhou, F.; Liu, W. High strength astringent hydrogels using protein as the building block for physically cross-linked multi-network. *ACS Appl. Mater. Interfaces* **2018**, *10* (9), 7593−7601.
(58) Xia, C.; Garcia, A. C.; Shi, S. Q.; Qiu, Y.; Warner, N.; Wu, Y.; Cai, L.; Rizvi, H. R.; D'Souza, N. A.; Nie, X. Hybrid boron nitride-natural fiber composites for enhanced thermal conductivity. *Sci. Rep.* **2016**, *6* (1), 34726.
(59) Smith McWilliams, A. D.; de Los Reyes, C. A.; Liberman, L.; Ergülen, S.; Talmon, Y.; Pasquali, M.; Martí, A. A. Surfactant-assisted individualization and dispersion of boron nitride nanotubes. *Nanoscale Adv.* **2019**, *1* (3), 1096−1103.
(60) Sileika, T. S.; Barrett, D. G.; Zhang, R.; Lau, K. H. A.; Messersmith, P. B. Colorless multifunctional coatings inspired by polyphenols found in tea, chocolate, and wine. *Angew. Chem., Int. Ed. Engl.* **2013**, *52* (41), 10766−10770.
(61) Lee, H.; Dellatore, S. M.; Miller, W. M.; Messersmith, P. B. Mussel-inspired surface chemistry for multifunctional coatings. *science* **2007**, *318* (5849), 426−430.
(62) Kwon, D.-J.; Wang, Z.-J.; Choi, J.-Y.; Shin, P.-S.; DeVries, K. L.; Park, J.-M. Interfacial and mechanical properties of epoxy composites containing carbon nanotubes grafted with alkyl chains of different length. *Composites, Part A* **2016**, *82*, 190−197.
(63) Chang, C.; Fennimore, A.; Afanasiev, A.; Okawa, D.; Ikuno, T.; Garcia, H.; Li, D.; Majumdar, A.; Zettl, A. Isotope effect on the thermal conductivity of boron nitride nanotubes. *Phys. Rev. Lett.* **2006**, *97* (8), 085901.
(64) Chen, Y.; Zou, J.; Campbell, S. J.; Le Caer, G. Boron nitride nanotubes: Pronounced resistance to oxidation. *Appl. Phys. Lett.* **2004**, *84* (13), 2430−2432.
(65) Wang, Y.-Z.; Gao, X.-F.; Liu, H.-H.; Zhang, J.; Zhang, X.-X. Green fabrication of functionalized graphene via one-step method and its reinforcement for polyamide 66 fibers. *Mater. Chem. Phys.* **2020**, *240*, 122288.
(66) Li, X.; Li, Y.; Alam, M. M.; Miao, J.; Chen, P.; Xia, R.; Wu, B.; Qian, J. Enhanced through-plane thermal conductivity in Polymer nanocomposites by constructing graphene-supported BN nanotubes. *J. Mater. Chem. C* **2020**, *8* (28), 9569−9575.
(67) Lee, D.; Song, S. H.; Hwang, J.; Jin, S. H.; Park, K. H.; Kim, B. H.; Hong, S. H.; Jeon, S. Enhanced mechanical properties of epoxy nanocomposites by mixing noncovalently functionalized boron nitride nanoflakes. *Small* **2013**, *9* (15), 2602−2610.
(68) Güzdemir, Ö.; Kanhere, S.; Bermudez, V.; Ogale, A. A. Boron nitride-filled linear low-density Polyethylene for enhanced thermal transport: continuous extrusion of micro-textured films. *Polymers* **2021**, *13* (19), 3393.
(69) Liu, Z.; Li, J.; Liu, X. Novel functionalized BN nanosheets/epoxy composites with advanced thermal conductivity and mechanical properties. *ACS Appl. Mater. Interfaces* **2020**, *12* (5), 6503−6515.
(70) Naderi, M.; Ebrahimi, F.; Najafi, M.; Naderi, H. Reinforcing effect of amine-functionalized and carboxylated porous graphene on toughness, thermal stability, and electrical conductivity of epoxy-based nanocomposites. *J. Appl. Polym. Sci.* **2019**, *136* (19), 47475.
(71) Yu, J.; Huang, X.; Wu, C.; Wu, X.; Wang, G.; Jiang, P. Interfacial modification of boron nitride nanoplatelets for epoxy composites with improved thermal properties. *Polymer* **2012**, *53* (2), 471−480.
(72) Martin-Gallego, M.; Hernández, M.; Lorenzo, V.; Verdejo, R.; Lopez-Manchado, M.; Sangermano, M. Cationic photocured epoxy

https://doi.org/10.1021/acsomega.4c05323
ACS Omega 2024, 9, 38946−38956

nanocomposites filled with different carbon fillers. *Polymer* **2012**, *53* (9), 1831−1838.
(73) Tang, L.-C.; Wan, Y.-J.; Yan, D.; Pei, Y.-B.; Zhao, L.; Li, Y.-B.; Wu, L.-B.; Jiang, J.-X.; Lai, G.-Q. The effect of graphene dispersion on the mechanical properties of graphene/epoxy composites. *Carbon* **2013**, *60*, 16−27.
(74) Shi, Z.; Li, X.-F.; Bai, H.; Xu, W.-W.; Yang, S.-Y.; Lu, Y.; Han, J.-J.; Wang, C.-P.; Liu, X.-J.; Li, W.-B. Influence of microstructural features on thermal expansion coefficient in graphene/epoxy composites. *Heliyon* **2016**, *2* (3), No. e00094.
(75) Liu, Y.; Zeng, K.; Zheng, S. Organic−inorganic hybrid nanocomposites involving novolac resin and polyhedral oligomeric silsesquioxane. *React. Funct. Polym.* **2007**, *67* (7), 627−635.
(76) Li, S.-Z.; Zhou, Y.-C.; Wang, L.-N.; Wang, S.-P.; Bai, L.; Feng, C.-P.; Bao, R.-Y.; Yang, J.; Yang, M.-B.; Yang, W. Flexible composite phase change materials with enhanced thermal conductivity and mechanical performance for thermal management. *J. Mater. Chem. A* **2023**, *11* (35), 18832−18842.
(77) Wu, J.; Song, X.; Gong, Y.; Yang, W.; Chen, L.; He, S.; Lin, J.; Bian, X. Analysis of the heat conduction mechanism for Al_2O_3/Silicone rubber composite material with FEM based on experiment observations. *Compos. Sci. Technol.* **2021**, *210*, 108809.
(78) Zhang, Z.; Li, M.; Wang, Y.; Dai, W.; Li, L.; Chen, Y.; Kong, X.; Xu, K.; Yang, R.; Gong, P.; et al. Ultrahigh thermal conductive polymer composites by the 3D printing induced vertical alignment of carbon fiber. *J. Mater. Chem. A* **2023**, *11* (20), 10971−10983.
(79) Li, X.; Wang, J.; Tian, Y.; Jiang, X.; Zhang, X. Thermal enhancement by constructing ordered-orienting hybrid network with modified boron nitride, graphene and carbon nanotubes in epoxy composite coatings. *Prog. Org. Coat.* **2022**, *172*, 107078.

https://doi.org/10.1021/acsomega.4c05323
ACS Omega 2024, 9, 38946−38956